

**Efficient Micro-Mixing of a Highly Viscous Bio-sample with Water
Using Orbital Shaking and Micro-Channels**

Liang Yuan

Department of Automation, Shanghai Jiao Tong University

Department of Electrical and Computer Engineering, The Ohio State University

Yuan F. Zheng

Department of Electrical and Computer Engineering, The Ohio State University

Weidong Chen

Department of Automation, Shanghai Jiao Tong University

(Dated: September 29, 2009)

ABSTRACT

Micro-mixing of a highly viscous bio-sample with water using orbital shaking and micro-channels is considered. Existing methods mix bio-samples by only shaking micro-wells or by specially designed micro-stirrers which are ineffective or inapplicable for highly viscous materials. Let alone small volumes at microliter or nanoliter level. Our method mixes a viscous bio-sample with water in micro-wells using orbital shaking plus an innovative block which divides the micro-wells into two compartments and is built in with micro-channels. The mixing method with the block in the micro-well is efficient compared with mixing in the micro-well without the block. In this paper, the design of the block is presented, the model of the flow of the bio-samples in the micro-channel is developed, the Reynolds number of the flow in the micro-channel is calculated, and the dynamics of the mixing process is analyzed. Furthermore, a miniature wireless video sensor system is used to observe the mixing process which verifies the model of the flow in the analysis. Finally, X-ray diffraction experiments on mixing monoolein with water are presented. In each trial, X-ray diffraction is used to evaluate the results of mixing which confirm that the proposed approach is effective for a mixing highly viscous bio-sample with water.

I. INTRODUCTION

In recent years, the technology of micro-mixing has attracted a great deal of attention due to its applications in analytical chemistry, food engineering, and life science. In the field of life science, for example, one application of micro-mixing is in the process of membrane protein crystallization, which is a necessary step for determining the structure of the protein using X-ray crystallography. It has been shown that crystallization of membrane protein is more difficult than that of regular proteins, which led to the invention of a special process called the in meso method which was proved effective for the purpose of crystal growth [1]. The method, however, requires a highly viscous lipid (monoolein) to be mixed with the protein solution (such as bacteriorhodopsin). Mixing in this manner produces a bio-sample having cubic phase structure, which is the medium required for crystal growth. According to the water-composition graph of the monoolein-water system shown in [2], the relevant phases such as the Pn3m cubic phase could form at 20°C when the weight of the water is between 39 and 41% (Fig. 1). The cubic phase is then dispensed into an array of wells on a plate as part of the crystallization setup [1, 3, 4]. The formed crystal can be used to determine the 3D structure of the protein using X-ray crystallography [5–7]. Moreover, a robotic system for automating the delivery of viscous bio-samples into arrays of wells has been built in our laboratory [8–12] which has significantly increased the efficiency and quality of dispensing. Unfortunately, the mixing of the lipid and protein solution was still done by hands using two micro-syringes [1]. Even worse is that this manual process must be done one sample at a time which is tedious and time-consuming.

In reviewing the literature, a number of methods for liquid mixing at the microliter level were found: micro-stirring, micro-well shaking, and mechanical-channels mixing. For micro-stirring, a device called micro-stirrer (agitator) has recently been invented [13–15], the major feature of which is that the agitator is a rotating magnet which drives the liquid instead of a mechanical bar immersed in the liquid. Micro-well plates can handle mixing at a very small scale ranging from 0.1mL to 5mL in each well, and orbital shaking of the entire plate is the most common method for mixing [16–18]. Unfortunately the micro-stirring and the micro-well shaking are still primarily used for handling low-viscous solutions such as bacteria, fungi, and yeasts as well as mammalian cells. Another method for liquid mixing is by mechanical channels which employ T-shape [19], Y-shape [20] and slit-type inter-digital homogenization [21], respectively. Those mechanical-channels are designed to mix low viscous liquids, which are pumped through the channels

continuously, and are not suitable for mixing highly viscous bio-samples at the microliter scale. In summary, the published literature suggests that mixing highly viscous ($> 3000\text{cP}$) and small volume bio-samples ($10\text{-}100\mu\text{L}$) represents a new and significant challenge.

In our previous work [22, 23], an approach for automatic mixing of highly viscous bio-samples was developed. It is to mix highly viscous bio-samples in microcapsules using a micro-channel with centrifugation. This paper presents a new approach for micro-mixing of small volumes of the same highly viscous bio-sample with water using micro-channels and orbital shaking. The new approach makes use of a small block, which is installed in the middle of the micro-well, and is built in with micro-channels. By using the continuous orbital motion, the bio-samples can flow in and out through the micro-channel to achieve mixing without using any moving parts to stir the samples.

The progress of this new approach was previously reported in two conference proceeding papers [24, 25]. In this archival journal paper, we document the details of the new approach particularly focusing on the physical insight of the mixing process through analysis, the detailed experimental setup for repeatability, and new experiments to formally verify the new approach. In addition, a comparable experiment without the block is conducted to verify the advantage of the new approach. Furthermore, a new sensing methodology which observes the mixing process online is introduced. The method is based a Miniature Wireless Video Sensor (MWVS) which is integrated into the plate of micro-wells as a whole such that the captured video is stationary in spite of the motion of the plate.

The paper is organized as follows. The design of the small block is introduced in Section II. The analysis of the mixing process in the micro-channel under the orbital force is presented in Section III. Observation of the mixing process with the MWVS is described in Section V. Experimental process and results using X-ray crystallography are presented in Section IV. Conclusions are given in Section V.

II. DESIGN OF THE BLOCK BUILT WITH MICRO-CHANNELS

In our new mixing mechanism the micro-well on a micro-well plate is divided into two compartments by a small block with micro-channels built in. The micro-well with the division has two functions. First, it houses the bio-samples such that the crystal can grow, and secondly it mixes the bio-samples by using the micro-channels. To accommodate the above two functions, the basic structure of the micro-well is shown in

Fig. 2. The unique feature is that a small block, which has the micro-channels built in, is installed in the middle of the micro-well. To achieve the effective mixing, the water in a compartment flows through the micro-channels to reach another compartment to mixing the highly viscous bio-sample under orbital shaking. Periodically, the water could continue to flow through the micro-channel until the homogeneous mixture is achieved.

In our design, the dimension of the micro-channel is considered due to the following reasons. Assume the volumes of the two bio-samples for mixing are V (microliters) each. The dimensions of the channel should guarantee the volume of V to flow through the micro-channel in a reasonably short period of time. Secondly, the long and narrow channel should be feasible to fabricate. Thirdly, the dimension should fit into the micro-well on the plate. Therefore, we have chosen the micro-channel to be 2mm long and 0.4mm in diameter for the targeted volume of $30\mu\text{L}$ in each bio-sample for the purpose of our application. The other dimensions of the small block, plus that of the micro-channel, are shown in Fig. 3. The 96 micro-wells plate with the small blocks, on the other hand, is designed for mixing bio-samples for the high-throughput purpose, as shown in Fig. 4. When the plate is in orbital shaking, centrifugal forces are generated which are applied to the samples in the micro-wells to drive them through the micro-channels for mixing.

To understand the channel-mixing, the type of flow should first be understood. In general, there are two types, laminar and turbulence. Laminar flow, which is characterized by smooth and constant fluid motion, occurs at low Reynolds numbers, where viscous forces are dominant, while turbulence flow occurs at high Reynolds numbers where inertial forces dominate. Turbulence flow is characterized by random eddies, vortices, and other flow fluctuations which the flow generates. Turbulence flow occurs in a large scale with a high Reynolds number and is more effective since the random eddies or vortices can increase greatly the inter facial area of two samples. Generally, micro-mixers are characterized by geometries with a low Reynolds number. In such micro-scale, turbulence flow is hard to achieve, especially, for highly viscous materials or low velocity, and mixing relies on diffusion [26]. However, if a special design is considered, such as a micro-channel, a driving agitator, or a magnetic bar, diffusion time could be reduced or turbulence may even be generated. In our designed block, the long and narrow channels are used for water to generate the turbulence. Under orbital shaking water initially contained in its own compartment flows

through the micro-channels to reach another compartment which contains the highly viscous bio-sample for the purpose of mixing. The water continuously flow back and forth between the two compartments through the micro-channels until it is homogeneously mixed into the highly viscous bio-samples.

The transition between laminar and turbulence flows is often indicated by a critical Reynolds number, which depends on the exact flow configuration and must be determined experimentally. Within a certain range around the critical number there is a region of gradual transition where the flow is neither fully laminar nor fully turbulence, and the prediction of the fluid behavior can be difficult. Generally within circular pipes the critical Reynolds number of 2300 is widely accepted. In the following section, Reynolds number in the micro-channel will be calculated such that the type of flow can be determined.

III. ANALYSIS OF THE MIXING PROCESS

As mentioned earlier, one important application of the current method is for crystallizing membrane proteins. Membrane protein crystallization uses a so-called in meso method. The method consists of the following two steps for growing crystals [2, 4]: (1) mix two parts protein solution/dispersion with three parts lipid (usually monoolein), by which the cubic phase forms spontaneously, (2) add precipitant/salt and incubate, by which crystals form in hours to weeks. All operations take place at 20°C [4, 27].

The key to the in meso method is the homogeneous mixing of protein with the lipid and the formation of the cubic phase. There are several types of the cubic phase, for example, Lc, L α , cubic-Ia3d, and cubic-Pn3m (Fig. 1), etc. Each has its own characteristic low-angle diffraction pattern under the X-ray [2] which is used to index the corresponding space group (Pn3m, Ia3d, etc). The cubic-Pn3m phase has been proven to be a useful medium for the growth of well-structured crystals of membrane proteins [28, 29].

In our work, we use pure water in lieu of membrane protein solution to mix with monoolein since the viscosity of the membrane protein solution is close to water [23]. If cubic-Pn3m can form using our mixing method, it should also be effective for mixing with the membrane protein solution. In that case, we could mix two parts water with three parts monoolein through micro-channels under the orbital shaking. The density of monoolein is similar to water, but its viscosity is very high ($> 10^5$ cP) and even much higher than honey (3, 000cP). Fundamentally, we need to understand how the viscous biosample mixes with water using the micro-channel under the orbital shaking to achieve mixing. To do so, a dynamical model of the

flow of the viscous materials in the orbital shaking needs to be built. To our knowledge, this model has never been established for the purpose of micro-channel mixing of viscous bio-samples using orbital motion.

It should be noted that there exist a crucial difference between the orbital and the rotational motions. In the orbital motion the orientation of the object maintains constant while it changes in the rotational motion. The details of the orbital movement and the relationship between neighboring points during the movement is shown in Fig. 5, in which the well is attached with the coordinates (x_2, y_2) and experiences a orbital motion, i.e., the orientations of x_2 and y_2 are constant when the well moves.

To understand the flow of the viscous materials in the micro-channel, the force exerted on the micro-channel, which is to be revealed by the following analysis, should be known first. For an orbital shaker, assume the radius of the orbital motion to be R and the rotation speed to be ω . The centrifugal force exerted at the center point of the axis of the micro-channel, denoted as $A(x, y)$, can be described by:

$$F = m\omega^2 d_{o_1A}. \quad (1)$$

where m is the mass of the entire bio-sample and d_{o_1A} is the distance from o_1 to A .

The driving force along the micro-channel for mixing the bio-samples as shown in Fig. 5 is given as:

$$F_t = F \sin \omega t_A = m\omega^2 d_{o_1A} \sin(\omega t - \theta), \quad (2)$$

where:

r is the vertical distance from the center of micro-well and the central axis of a micro-channel;

θ is the angle between o_1o_2 and o_1A ;

$$d_{o_1A} = \sqrt{R^2 + r^2 + 2Rr \cos \omega t}.$$

Practically, r is much smaller in comparison with R ; therefore, one may consider $\omega t - \theta \approx \omega t$. Consequently, the driving force can be expressed as:

$$F_t = m\omega^2 d_{o_1A} \sin \omega t. \quad (3)$$

From equation (3), one can see that the driving force alternates periodically. When $\omega t = 0$ which means that the well is on the top of the circle, the driving force is equal to zero; when the well is on the far left or right, the driving force reaches the maximum. The average driving force can be derived as follows.

$$\bar{F}_t = m\omega^2 \bar{d}. \quad (4)$$

where \bar{d} is the average value of $d_{oLA}\sin\omega t$ in the period of and can be expressed as:

$$\bar{d} = \frac{2}{\pi} \int_0^{\pi/2} \sin \omega t \sqrt{R^2 + r^2 + 2Rr \cos \omega t} d\omega t = \frac{2[(R+r)^2 - (R^2 + r^2)^{3/2}]}{3\pi Rr}. \quad (5)$$

If r is so small in comparison with R , \bar{d} can be further approximated as

$$\bar{d} = \frac{2R}{\pi}. \quad (6)$$

With the average driving force expressed as equation Eq. (4), we are ready to derive the average speed of the flow of the viscous materials in the micro-channel.

From our previous studies [22, 23], it was obtained that the relationship between the driving force and the speed of the flow of the viscous materials in the micro-channel can be expressed as:

$$\bar{v} = \frac{F_t}{32\pi l \mu}. \quad (7)$$

where l the length of the micro-channel. By using Eq. (4), Eq. (7) becomes:

$$\bar{v} = \frac{m\omega^2 \bar{d}}{32\pi l \mu} = \frac{\rho V \left(\frac{2\pi}{60}\right)^2 n^2 \bar{d}}{32\pi l \mu} = \frac{1.09 \times 10^{-4} \rho V n^2 \bar{d}}{\mu l}, \quad (8)$$

where n is the speed of spin of the orbital shaker (rpm) and V is the volume of the bio-sample. Accordingly, the Reynolds number under the orbital shaking force can be calculated as:

$$R_e = \frac{2\bar{v}\rho r_c}{\mu} = \frac{2.18 \times 10^{-4} \rho^2 r_c n^2 \bar{d}}{\mu^2 l}, \quad (9)$$

where r_c is the radius of the micro-channel. In the experiment, we use the Thermo Forma Orbital Shaker of which the maximum shaking speed is 525rpm, which is used to generate the turbulence and the radius of the orbital motion R is 25mm. Also r can be set as 3.0mm, 2.4mm, 1.6mm, 1.0mm, or 0.4mm for different micro-channels on the block, according to the design as shown in Fig. 3. The corresponding values of \bar{d} are between 16.1mm and 16.9mm, which are close to each other since R is much larger than r . For simplification, we set \bar{d} as 16.5mm. Given $l=2\text{mm}$, $\mu=1.0 \times 10^{-3} \text{ Pa}\cdot\text{s}$, $\rho=0.98 \times 10^3 \text{ kg/m}^3$, and $r_c=0.2\text{mm}$, the 30 μL water flowing through the micro-channel has a Reynolds numbers of 2,928 with $n=525\text{rpm}$, which represent a turbulence flow. But monoolein has a small Reynolds number (less than 100) due to its

high viscosity. In fact, monoolein is so sticky that it cannot flow through the micro-channels under the maximum shaking speed of a regular shaker (525rpm).

For effective mixing, the water is dispensed into one compartment, and the monoolein into the other as shown in Fig. 6. Under orbital shaking, the water flows into the monoolein compartment through the micro-channels. Due to the turbulence flow, the water will jet into the monoolein by a large number of eddies and vortices to smash the monoolein. Since monoolein has a hydrophilic region in the molecular structure [1], it could be diffused with water for mixing. However, the monoolein cannot flow through the micro-channels into the water compartment due to its high viscosity. After the initial mixing, the remaining free water will flow back to its own compartment through the channels on the other side of the block and continue to jet into the monoolein compartment again and again for smashing the monoolein. In this way, the water repeats to flow in and out the monoolein compartment under the orbital shaking until effective mixing is achieved. If the micro-channels on one side of the block are sealed to prevent the water from flowing back, which means that water can flow in the monoolein compartment only once, the water will only smash the monoolein once. Under this condition, the mixing cannot be effectively done, which will be shown later in this paper. Therefore, the micro-channels of both sides of the block are necessary for the mixing. An MWVS is used to observe the mixing processes with different conditions to prove the above analysis, which will be shown in the following section.

IV. OBSERVATION OF THE MIXING PROCESS WITH A MINIATURE WIRELESS VIDEO SENSOR

To reveal the mixing process of a highly viscous biosample with water, the MWVS is used to observe the micro-well. For evaluating the mixing quantitatively with the video sensor, dye water is used to mix with the monoolein instead of purified water.

A. Experiment preparation and method

1. Shaker

A Thermo Forma orbital shaker was used to generate the centrifugal force. The radius of the orbital motion is 25mm. The maximum speed is 525rpm, which was used in our experiment. The temperature ranges from 5°C to 60°C.

2. Micro-well plate

A standard 96 well plate with flat bottom (SARSTEDT, Newton, NC) was used. The well has a diameter of 6.8mm and a depth of 10mm. The small block is as long as the diameter of the well, as tall as the depth of the well, and as thick as 2mm. There are 16 micro-channels distributed on the block as shown in Fig. 3. The diameter of the micro-channel is 0.4mm. The plate was covered with a 1mm-thick plastic lid during the mixing.

3. Materials

Monoolein (1-oleoyl-rac-glycerol, lot M-239-M8-R) was purchased from Nu Chek Prep Inc. (Elysian, MN). It had a purity of > 99% as determined by thin layer chromatography and was used without further purification. Dye (Bromophenol Blue Sodium Salt) was purchase from USB Corporation (Cleveland, OH).

4. Video sensor system

In general, it is desirable to observe the mixing process in real-time [30, 31]. The challenge is that the plate is in motion. To capture the process in image it is necessary to use a camera with extremely short exposure time if the camera system is stationary (100 ns) [30]. Furthermore, the mechanical structure for installing such a camera system will be very complicated. Apparently a stationary camera system will be expensive. Our innovation is to use a miniature video sensor which is structurally integrated it into the plate as a whole such that the sensor moves with the micro-well being observed. As a result, a simple and low-cost video sensor can be used, instead of a complicated and expensive one, to observe the mixing process. For the purpose, an MWVS system is used. The system includes the MWVS (Q-See[®] miniature wireless camera with a receiver, model: QSWLMCR), a USB DVR (Q-See[®] 4 channels DVR, model: QSU2DVR04), and a PC. The flow chart of the observation system is shown in Fig. 7. The wireless video sensor captures and transmits the sample images to the wireless receiver with 2.4GHz wireless transmission. USB DVR converts the video analog signal from the wireless receiver to the digital signal for computer recording. The display and recording rate of USB DVR is 30fps.

5. Installation of the MWVS on the plate

The MWVS needs to be installed on the 96 well plate. In the installation, the sensor has to focus on the bottom of the well where the mixing takes place. A transparent spacer is designed to adjust the distance from the sensor to the samples and is also used to support the sensor on the plate. All the components are

integrated together by glue and tape as a whole. Fig. 8 shows the installation of the MWVS on the 96 well plate.

B. Experimental results

Image acquisition was used to monitor and analyze the mixing process. Fig. 9 shows the mixing process without the block in a well. The water and monoolein are delivered into the well and attempt to mix through the shaking. The experiment shows that even after 30min, the color of the dye water is not uniformly distributed with the monoolein, which means that mixing cannot be done in as long as 30min. Fig. 10 shows the mixing process with the block in place. The process is shown every 10sec or so until 60sec elapse. One can see that within 60sec, the mixing is well achieved by seeing the uniform color at the bottom of the well. Note that only the monoolein compartment (half of the well) is shown in the figure. Furthermore, each captured image is converted into an 8-bit grey-scale bitmap (0-255) shown in Fig. 10. These bitmaps are transformed into an intensity histogram representing the full area of the mixing compartment. In the figure, the unit of the horizontal axis is Pixel Intensity, and that of the vertical axis is the number of pixels. If the mixing is completely homogeneous, the bitmap should show an impulse at a particular Pixel Intensity. Naturally when the standard deviation σ becomes smaller, the mixing is getting more homogeneous.

V. X-RAY DIFFRACTION EXPERIMENT

The purpose of the X-ray diffraction experiment is to test the effectiveness of our method for a homogenous mixing. For evaluating the result of mixing, X-ray crystallography was used to test the form of the cubic phase. In each time of the testing, four samples are randomly taken from the mixture which resides in a single micro-well. If the mixing is homogeneous, the four samples should produce the same diffraction pattern; otherwise, the patterns will be different which means that the mixing is not completed.

A. Experiment preparation and method

1. X-ray machine

X-ray diffraction measurements were performed using a rotating anode x-ray generator (Rigaku RU-H3R operating at 40kV and 90mA) which produced Cu radiation (wavelength $\lambda = 1.5418 \text{ \AA}$). Detector was R-AXIS IV++ which combined two large active area (300mm \times 300mm) imaging plates with fast readout

speeds and a wide dynamic range, making it ideal for collecting accurate diffraction data. Crystal to detector distance was 450mm.

2. Sample preparation for X-ray diffraction

30 μ L monoolein was dispensed in one half of a micro-well and 30 μ L water was in the other. The micro-well plate was put in the orbital shaker (Thermo Forma Orbital Shaker) for mixing. Mixing was carried out at room temperature (20 °C). The mixed samples were transferred to 0.3mm diameter quartz capillaries (Charles Supper, Natick, MA) and wax-sealed for examining.

3. X-ray diffraction of mixture

For cubic liquid crystalline phase, it has $d_{hkl}=a_0/(h^2+ k^2 + l^2)^{1/2}$, ratio 1, $\sqrt{2}$, $\sqrt{3}$, $\sqrt{4}$, $\sqrt{5}$, $\sqrt{6}$, $\sqrt{8}$, and $\sqrt{9}$ which are indexed as (100), (110), (111), (200), (210), (211), (220), and (221)/(300) reflection, respectively. In these equations, d_{hkl} is the spacing of the set of lattice planes (h , k , l) characterized by the Miller indices h , k , and l ; a_0 is the lattice spacing of the cubic phase. For different crystals, there are different Miller indices which denote planes and their corresponding directions in X-ray crystallography, which is a unique and effective tool for revealing the crystal structures [1]. The reflections of the different planes and their relative positions are displayed in the crystallography. For bicontinuous cubic phases, Pn3m and Ia3d for example, their indices have been found. For Pn3m, the sequence of the allowed reflections is $hkl=110$, 111, 211, 221/300, etc, and the relative peak positions are $\sqrt{3}$, $\sqrt{6}$, and $\sqrt{9}$, etc [32].

B. Experimental results

In our experiment, the experiments of the mixing without and with the block were implemented in order to evaluate the effect of the mixing block. The experiment of the mixing with sealed eight channels on one side of the block was also implemented. The results presented below concern the mixing effects without the block and with the block. The phase characteristics were quantified by low angle X-ray diffraction. Four small samples were randomly taken from the mixture in a single micro-well for testing. If the cubic phase is evenly mixed, all the four samples should produce the same diffraction pattern.

1. Mixing without the block

To verify our new method, mixing monoolein with water without the block was tested. When spin speed $n=525$ rpm and shaking time $t=30$ min, the patterns of the four samples represent two different phases: Pn3m

and Pn3m+Ia3d, which means that monoolein has not been mixed well with water. The results are shown in Fig. 12 and Table I.

TABLE I: X-ray diffraction of $n=525\text{rpm}$, $t=30\text{min}$ without the block

Samples	$d(\text{\AA})(^\circ)$	hkl	$a_0(\text{\AA})$	Space group
(a)	72.09(1.2 $^\circ$)	110	101.9	Pn3m
	58.71(1.4 $^\circ$)	111	101.6	
	41.31(2.1 $^\circ$)	211	101.2	
	33.62(2.6 $^\circ$)	221/300	100.9	
			101.4(1.3%)	
(b)	72.63(1.3 $^\circ$)	110	102.7	Pn3m
	59.40(1.4 $^\circ$)	111	102.8	
	42.38(2.1 $^\circ$)	211	103.8	
	34.64(2.7 $^\circ$)	221/300	103.9	
			103.3(2.3%)	
(c)	70.43(1.2 $^\circ$)	110	99.6	Ia3d+Pn3m
	59.09(1.6 $^\circ$)	111	102.3	
	41.90(2.4 $^\circ$)	211	102.6	
	34.22(2.7 $^\circ$)	221/300	102.7	
(d)	68.92(1.3 $^\circ$)	110	97.4	Ia3d+Pn3m
	58.51(1.5 $^\circ$)	111	101.8	
	41.99(2.5 $^\circ$)	211	102.8	
	35.13(2.8 $^\circ$)	221/300	105.9	

2. Mixing with the block

This experiment is to discover the effectiveness of mixing with the blocks when all of the channels are opened and half of the channels are sealed, respectively. First of all, the experiment with all the micro-channels opened is implemented with the duration of shaking decreased to $t=2\text{min}$ and 1min at 525rpm , respectively. All the results are Pn3m, as shown in Fig. 13 and Table II, and Fig. 14 and Table III, respectively. Next, the returning micro-channels on one side of the block are sealed, and the patterns of the four samples demonstrate two different phases: Ia3d and Pn3m, as shown in Fig. 15 and Table IV, which means that the cubic phase has not been evenly mixed. Therefore, the block needs all the micro-channels on both sides for the water to flow back and forth; otherwise, mixing cannot be effectively achieved.

TABLE II: X-ray diffraction of $n=525\text{rpm}$, $t=2\text{min}$ with the block

Samples	$d(\text{\AA})(^\circ)$	hkl	$a_0(\text{\AA})$	Space group
(a)	70.62(1.1 $^\circ$)	110	99.9	Pn3m
	57.69(1.4 $^\circ$)	111	99.9	
	40.91(2.0 $^\circ$)	211	100.2	
	33.39(2.7 $^\circ$)	221/300	100.1	
			100.0(0.5%)	
(b)	69.32(1.4 $^\circ$)	110	98.0	Pn3m
	57.43(1.6 $^\circ$)	111	99.4	
	40.12(2.2 $^\circ$)	211	98.3	
	32.73(2.7 $^\circ$)	221/300	98.2	
			98.5(1.9%)	
	69.92(1.3 $^\circ$)	110	98.9	
	57.46(1.5 $^\circ$)	111	99.5	

(c)	40.16(2.1°)	211	98.4	Pn3m
	32.99(2.6°)	221/300	98.9 98.8(1.1%)	
(d)	69.93(1.2°)	110	98.9	Pn3m
	57.12(1.6°)	111	98.9	
	40.66(2.0°)	211	99.6	
	33.10(2.4°)	221/300	99.3 99.2(1.1%)	

TABLE III: X-ray diffraction of n=525rpm, t=1min with the block

Samples	d(Å)(°)	hkl	a ₀ (Å)	Space group
(a)	70.03(1.1°)	110	99.0	Pn3m
	57.60(1.3°)	111	99.9	
	40.82(2.2°)	211	100.0	
	33.16(2.8°)	221/300	99.5 99.8(1.4%)	
(b)	69.33(1.3°)	110	98.0	Pn3m
	57.24(1.6°)	111	98.3	
	40.82(2.1°)	211	99.8	
	33.02(2.6°)	221/300	99.1 99.1(1.8%)	
(c)	69.42(1.3°)	110	98.2	Pn3m
	57.18(1.5°)	111	99.0	
	40.16(2.2°)	211	98.4	
	32.76(2.6°)	221/300	98.3 98.5(1.1%)	
(d)	69.92(1.3°)	110	98.9	Pn3m
	57.46(1.7°)	111	99.5	
	40.16(2.3°)	211	98.4	
	33.99(2.8°)	221/300	98.9 98.9(1.1%)	

TABLE IV: X-ray diffraction of n=525rpm, t=1min with the half sealed channels

Samples	d(Å)(°)	hkl	a ₀ (Å)	Space group
(a)	71.52(1.2°)	110	101.1	Pn3m
	59.09(1.5°)	111	102.3	
	41.59(2.1°)	211	101.9	
	34.32(2.7°)	221/300	102.9 102.0(2.1%)	
(b)	71.90(1.2°)	110	101.7	Ia3d+Pn3m
	59.37(1.5°)	111	102.8	
	42.58(2.1°)	211	104.3	
	35.38(2.5°)	221/300	106.1	
(c)	69.56(1.3°)	110	98.4	Ia3d+Pn3m
	59.07(1.5°)	111	102.8	
	41.48(2.1°)	211	104.3	
	34.81(2.5°)	221/300	106.1	
(d)	67.84(1.3°)	110	95.9	Ia3d+Pn3m
	58.33(1.5°)	111	101.0	
	41.41(2.1°)	211	101.4	
	34.54(2.6°)	221/300	103.6	

VI. CONCLUSIONS

Mixing highly viscous bio-samples at the microliter level presents a new and significant challenge to the instrumentation field. In this paper, a novel mechanism for micro-mixing of a highly-viscous bio-sample with water using orbital shaking and micro-channels is presented. The design of a small block which has micro-channels built in on both sides of the block is described. The small block is to divide the micro-well into two compartments, while the micro-channels allow water to travel between the two compartments for the purpose of mixing. To understand the micro-channel mixing with shaking, the Reynolds number is derived based on the dimension of the micro-channels. Then the dynamics of the mixing process is analyzed. According to the Reynolds number, the micro-channel generates turbulence flow for the water, which is responsible for the mixing of the highly viscous material. The dynamic process reveals how fast the water can go through the micro-channel under the motion of shaking which may lead to the design of the speed and duration of the spin of the shaker. To observe the micro-channel mixing with shaking, a Miniature Wireless Video Sensor is used. According to the captured pictures in the mixing process, the micro-channel generates jet flow for the water, which is responsible for mixing itself with the highly viscous material. Also, water flowing back and forth between the two compartments is a key factor for an effective and efficient mixing. Furthermore, X-ray diffraction experimental results show that the new mixing method is valid, and verify that $n=525\text{rpm}$ and $t=1\text{min}$ is an optimal set of parameters for a homogeneous mixing of monoolein and water using the standard 96 well plate.

REFERENCES

- [1] M. Caffrey, *J. Struct. Biol.* 142, 108 (2003).
- [2] J. Briggs, H. Chung, and M. Caffrey, *J. Phys. II France* 6, 723 (1996).
- [3] V. Cherezov and M. Caffrey, *J. Appl. Cryst.* 38, 398 (2005).
- [4] E. Landau and J. Rosenbusch, in *Proc. National Academy of Science* 14532 (1996).
- [5] V. Luzzati, *Physical Facts and Functions* 1, 71 (1968).
- [6] A. Michetts and S. Pfuntsch, *John Wiley & Sons* (1996).
- [7] M. Caffrey, *Membranes, Metabolism and Dry Organisms*, Edited by A. Leopold, New York: Cornell University Press, 350 (1986).

- [8] V. Cherezov, A. Peddi, L. Muthusubramaniam, Y. F. Zheng, and M. Caffrey, *Acta. Cryst. D* 60, 1795 (2004).
- [9] A. Peddi, L. Muthusubramaniam, Y. F. Zheng, V. Cherezov, and M. Caffrey, *IEEE Trans. on Automation Science and Engineering* 4(2), 129 (2007).
- [10] W. Chen, A. Peddi, Y. F. Zheng, and M. Caffrey, in *Proc. the 5th World Congress on Intelligent Control and Automation* 4650 (2004).
- [11] A. Peddi, Y. F. Zheng, V. Cherezov, and M. Caffrey, in *Proc. 2004 IEEE/RSJ International Conference on Intelligent Robots and Systems* 1282 (2004).
- [12] A. Peddi, Y. F. Zheng, V. Cherezov, and M. Caffrey, in *Proc. IEEE Conference on Automation Science and Engineering* 61 (2005).
- [13] S. R. Lamping, H. Zhang, B. Allen, and P. A. Shamlou, *Chem. Eng. Sci.* 58, 747 (2003).
- [14] J. Betts and F. Baganz, *Microb. Cell Fact.* 5, 1 (2006).
- [15] J. Buchs, *Biochem. Eng. J.* 7, 91 (2001).
- [16] <http://www.dasgip.de/>
- [17] <http://www.bioxplore.net/>
- [18] M. Micheletti, T. Barrett, S. D. Doig, F. Baganz, M. S. Levy, and G. J. Lye, *Chem. Eng. Sci.* 61, 2939 (2006).
- [19] A. Kawai, T. Futami, H. Kiriya, K. Katayama, and K. Nishiawa, *Micro-TAS* 1, 368 (2002).
- [20] T. Thorson, R. W. Roberts, F. H. Arnold, and S. R. Quake, *Phys. Rev. Lett.* 86, 4163 (2001).
- [21] K. Mae, T. Maki, I. Hasegawa, U. Eto, Y. Mizutani, and N. Honda, *Chem. Eng. J.* 101, 31 (2004).
- [22] L. Yuan, Y. F. Zheng, W. Chen, and M. Caffrey, in *Proc. IEEE Conference on Automation Science and Engineering* 634 (2007).
- [23] L. Yuan, Y. F. Zheng, and W. Chen, in *Proc. IEEE Conference on Automation Science and Engineering* 900 (2008).
- [24] L. Yuan, Y. F. Zheng, and W. Chen, in *Proc. IEEE Conference on Robotics and Biomimetics* 1236 (2008).
- [25] L. Yuan and Y. F. Zheng, in *Proc. IEEE Conference on Automation Science and Engineering* 579 (2009).

- [26] P. Graveson, J. Branbjerg, and O.S. Jensen, *J. of Micromech. and Microeng.* 3, 168 (1993).
- [27] E. Landau, G. Rummel, S. Cowan-Jacob, and J. Rosenbusch, *J. of Phys. Chem. B* 101, 1935 (1997).
- [28] M. Chiu, P. Nollert, M. Loewen, H. Belrhali, E. Pebay Peyroula, J. Rosenbusch, and E. Landau, *Acta Cryst. D* 56, 781 (2000).
- [29] P. Nollert, H. Qiu, M. Caffrey, J. Rosenbusch, and E. Landau, *FEBS Lett.* 504, 179 (2001).
- [30] M. Grumann, A. Geipel, L. Riegger, R. Zengerle, and J. Ducree, *Lab on a Chip* 5, 560 (2005).
- [31] V. Hessel, H. Lowe, and F. Schonfeld, *Chem. Eng. Sci.* 60, 2479 (2005).
- [32] K. Larsson, *Nature* 304, 664 (1983).

Figure Captions

FIG. 1: Water-composition phase diagram for the monoolein water system [1], where L_c , $L\alpha$, $Ia3d$, FI , and $Pn3m$ are various cubic phases.

FIG. 2: Micro-well divided by a small block with micro-channels built in (top view).

FIG. 3: The dimension of the small block: (a) top view, and (b) side view where the units are in mm. Note that the 16 micro-channels are on the bottom of the micro-well with 8 on each side of the block.

FIG. 4: The 96 micro-wells plate with the small blocks in each micro-well shaking in an orbital shaker.

FIG. 5: The model of the orbital shaking.

FIG. 6: Mixing monoolein with water in the micro-well divided by a block.

FIG. 7: The block diagram of the video sensor system.

FIG. 8: Installation of the MWVS on the 96-well plate.

FIG. 9: Evaluation of the mixing process without the block. The images show the mixing process starting from 0 min to 30 min: (a) 0 min, (b) 5 min, (c) 10 min, (d) 15 min, (e) 20 min, (f) 25 min, and (g) 30 min.

FIG. 10: Evaluation of the mixing process with the block. The images show the mixing process in the compartment of monoolein starting from 0 sec to 60 sec: (a) 0 sec, (b) 12 sec, (c) 24 sec, (d) 31 sec, (e) 44 sec, (f) 50 sec, and (g) 60 sec.

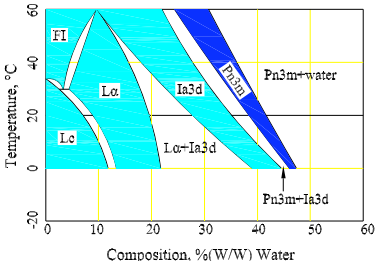
FIG. 11: The corresponding 2D-histograms at different times and its standard deviation (σ) of the mixing process with the block: (a) 12 sec and $\sigma = 31.48$, (b) 24 sec and $\sigma = 31.48$, (c) 31 sec and $\sigma = 30.06$, (d) 44 sec and $\sigma = 30.06$, (e) 50 sec and $\sigma = 22.59$, (g) 60 sec and $\sigma = 21.61$. The unit of the horizontal axis is Pixel Intensity, and that of the vertical axis is the number of pixels.

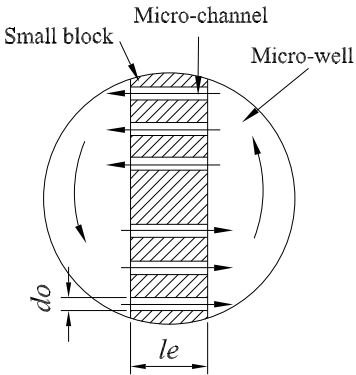
FIG. 12: Low-angle X-ray diffraction patterns of the four samples taken from the mixed cubic phase in a single micro-well at $n=525$ rpm and $t=30$ min without the block: (a) and (b) $Pn3m$, (c) $Pn3m+Ia3d$, (d) $Pn3m+Ia3d$.

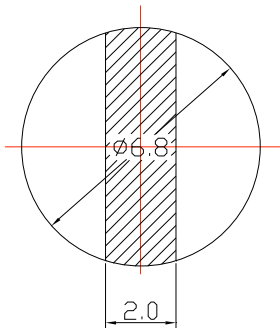
FIG. 13: Low-angle X-ray diffraction patterns of the four samples taken from the mixed cubic phase in a single micro-well at $n=525$ rpm and $t=2$ min with the block. All shows $Pn3m$.

FIG. 14: Low-angle X-ray diffraction patterns of the four samples taken from the mixed cubic phase in a single micro-well at $n=525$ rpm and $t=1$ min with the block. All shows $Pn3m$.

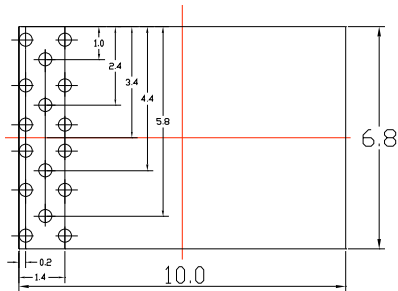
FIG. 15: Low-angle X-ray diffraction patterns of the four samples taken from the mixed cubic phase in a single micro-well at $n=525$ rpm and $t=1$ min with half sealed channels: (a) $Pn3m$, (b), (c) and (d) $Ia3d+Pn3m$.



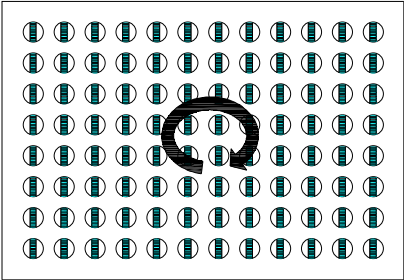




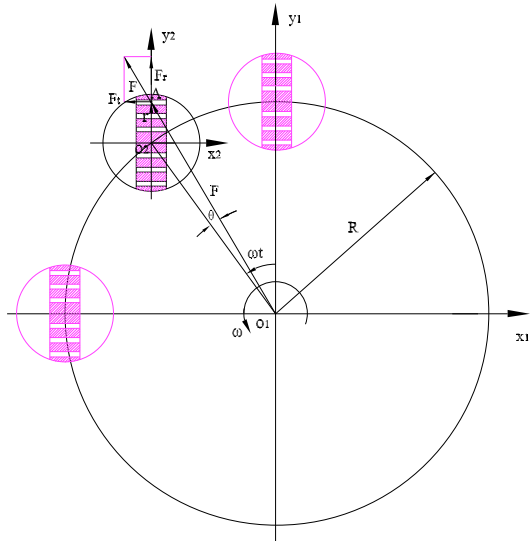
(a)

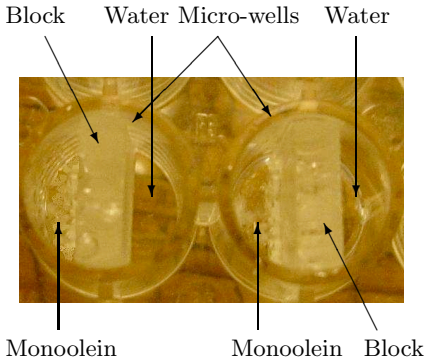


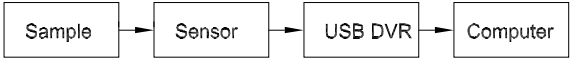
(b)



shaking





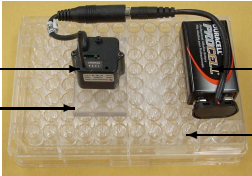


Wireless sensor

Spacer

Battery

Plate





(a)



(b)



(c)



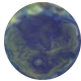
(d)



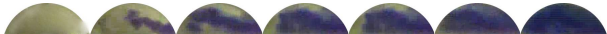
(e)



(f)



(g)



(a)

(b)

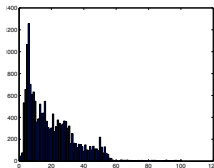
(c)

(d)

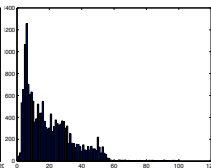
(e)

(f)

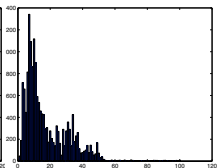
(g)



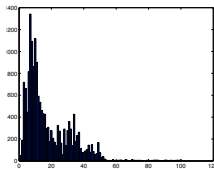
(a)



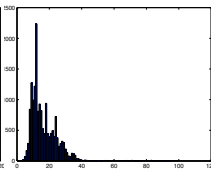
(b)



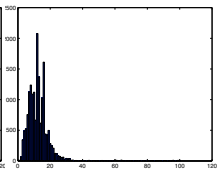
(c)



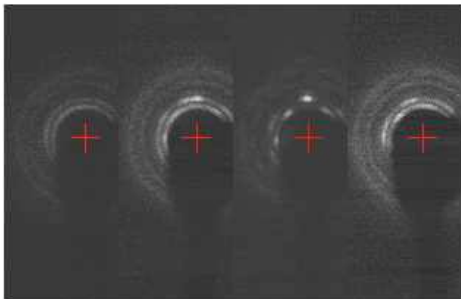
(d)



(e)



(f)

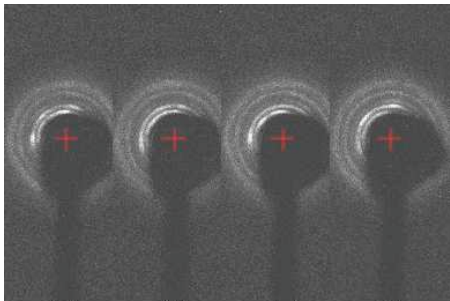


(a)

(b)

(c)

(d)

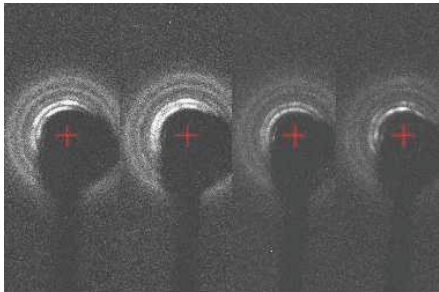


(a)

(b)

(c)

(d)

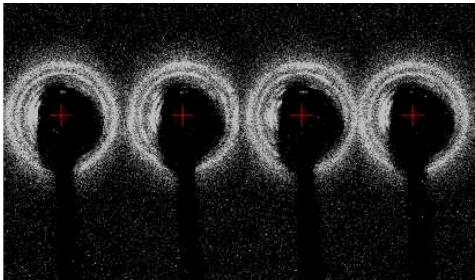


(a)

(b)

(c)

(d)



(a)

(b)

(c)

(d)